Effects of Reversing the Protein Positive Charge in the Proximity of the Flavin N(1) Locus of Choline Oxidase[†]

Mahmoud Ghanem[‡] and Giovanni Gadda*[,‡,§]

Departments of Chemistry and Biology and The Center for Biotechnology and Drug Design, Georgia State University, Atlanta, Georgia 30302-4098

Received December 9, 2005; Revised Manuscript Received January 11, 2006

ABSTRACT: A protein positive charge near the flavin N(1) locus is a distinguishing feature of most flavoprotein oxidases, with mechanistic implications for the modulation of flavin reactivity. A recent study showed that in the active site of choline oxidase the protein positive charge is provided by His_{466}. Here, we have reversed the charge by substitution with aspartate (CHO-H466D) and, for the first time, characterized a flavoprotein oxidase with a negative charge near the flavin N(1) locus. CHO-H466D formed a stable complex with choline but lost the ability to oxidize the substrate. In contrast to the wild-type enzyme, which binds FAD covalently in a 1:1 ratio, CHO-H466D contained ∼0.3 FAD per protein, of which 75% was not covalently bound to the enzyme. Anaerobic reduction of CHO-H466D resulted in the formation of a neutral hydroquinone, with no stabilization of the flavin semiquinone; in contrast, the anionic semiquinone and hydroquinone species were observed with the wild type and a H466A variant of the enzyme. The midpoint reduction potential for the oxidized−reduced couple in CHO-H466D was ∼160 mV lower than that of the wild-type enzyme. Finally, CHO-H466D lost the ability to form complexes with glycine betaine or sulfite. Thus, with a reversal of the protein charge near the FAD N(1) locus, choline oxidase lost the ability to stabilize negative charges in the active site, irrespective of whether they develop on the flavin or are borne on ligands, resulting in defective flavinylation of the protein, the decreased electrophilicity of the flavin, and the consequent loss of catalytic activity.

The presence of a protein positive charge proximal to the N(1) locus of the flavin was proposed in flavoprotein oxidases long before the three-dimensional structures of a number of flavin-dependent oxidases had become available (*1*−*5*). Indeed, most flavoprotein oxidases thermodynamically stabilize the anionic flavin semiquinone (*6*−*11*), form a stable reversible N(5) flavin adduct with sulfite (*1*−*4*, *6*, *7*, *11*−*13*), and stabilize the benzoquinoid anion forms of 6-hydroxy-, 8-hydroxy-, 6-mercapto-, and 8-mercaptoflavin analogues (*4*, *14*−*17*), all features that require the stabilization of a negative charge localized in the N(1)−C(2)═O region of the flavin. The mechanistic implications for a protein positive charge stabilizing a negative charge on the N(1) locus of the flavin are (i) to render flavin reduction thermodynamically favorable by elevating the midpoint reduction−oxidation potential of the bound flavin (*1*, *4*, *15*, *17*−*19*), (ii) to preferentially stabilize the anionic form of the reduced flavin that readily reacts with oxygen (*1*−*4*, *18*, *19*), and (iii) to facilitate the flavinylation process for those enzymes in which the flavin is covalently linked to the protein moiety (*20*). To date, the X-ray crystallographic structures of glucose oxidase from *Aspergillus niger* (*21*) and *Penicillium amagasakiense* (*22*), cholesterol oxidase from *Brevibacterium sterolicum* (*23*) and *Streptomyces* sp. (*24*, *25*), pyranose 2-oxidase from *Peniophora* sp. (*26*) and *Trametes multicolor* (*27*), cellobiose dehydrogenase from *Phanerochaete chrysosporium* (*28*), baker's yeast flavocytochrome b_2 (*29*), spinach glycolate oxidase (*30*), pig kidney D-amino acid oxidase (*31*), and bacterial sarcosine oxidase (*32*), trimethylamine dehydrogenase (*33*), and dihydroorotate dehydrogenase (*34*) have shown that either a positively charged amino acid residue or a dipole of an α-helix is oriented toward the N(1)−C(2)═O region of the enzyme-bound flavin. While the effects of replacing the positive charge with a neutral amino acid on the flavin properties have been investigated for lactate monooxygenase (*35*), no studies have addressed the characterization of the flavin properties of an oxidase in which the positive charge close to the flavin N(1) locus was reversed.

Choline oxidase (EC 1.1.3.17) is a flavin-dependent enzyme that oxidizes choline to glycine betaine via an enzyme-bound aldehyde intermediate (Scheme 1). This reaction is of considerable interest for medical and biotechnological applications, since accumulation of glycine betaine in many pathogens and plants enables their stress resistance toward hyperosmotic environments (*36*, *37*). Choline oxidase has been characterized in its biophysical, structural, and mechanistic properties. The enzyme is a homodimer with a

[†] This work was supported in part by Grant PRF 37351-G4 and Grant PRF 47363-AC4 from the American Chemical Society and a Research Initiation Grant from Georgia State University (G.G.). M.G. thanks the Egyptian Government for its continuous financial support.

* To whom correspondence should be addressed: Department of Chemistry, Georgia State University, P.O. Box 4098, Atlanta, GA 30302-4098. Phone: (404) 651-4737. Fax: (404) 651-1416. E-mail: ggadda@gsu.edu.

[‡] Department of Chemistry.

[§] Department of Biology and The Center for Biotechnology and Drug Design.

10.1021/bi052514m CCC: $33.50
Published on Web 02/18/2006

Scheme 1

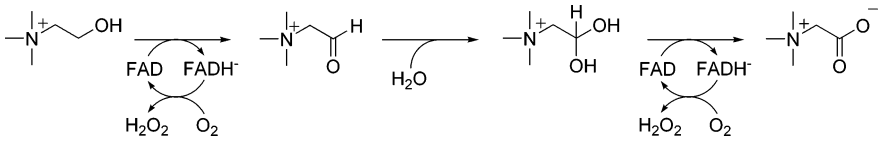

Scheme 2

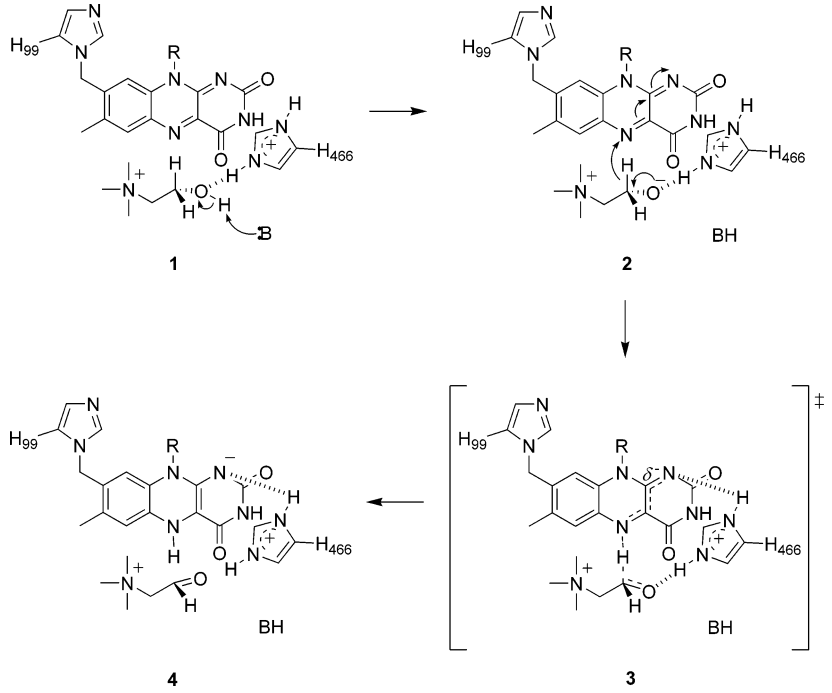

mass of 120 kDa (*38*), contains covalently linked FAD in a 1:1 stoichiometry (*38*), and under turnover cycles between its fully oxidized and reduced states (*39*, *40*). A detailed picture of the catalytic mechanism of choline oxidase has emerged from pH, kinetic isotope, and temperature effect studies (*39*−*43*), as well as mechanistic studies with substrate and product analogues (*44*) and site-directed mutants (*45*). Briefly, in catalysis an unidentified active site base with a pK_a of 7.5 activates the alcohol substrate with formation of an alkoxide species (species 1 in Scheme 2) (*39*), which is transiently stabilized in the active site through electrostatic interaction with the imidazolium side chain of His_{466} (*45*) (species 2 and 3 in Scheme 2). Transfer of a hydride from the α-carbon of the substrate to the enzyme-bound flavin occurs quantum mechanically from the activated choline alkoxide species (species 3 in Scheme 2) (*39*, *41*). Substrate binding is mainly dictated by interactions involving the trimethylammoniun headgroup of the alcohol, with little participation of the ethyl moiety (*44*). In a recent study in which His_{466} was replaced with alanine, our group showed that in catalysis His_{466} is protonated and that, besides stabilizing the transient alkoxide species that is formed in catalysis, this protein group modulates the electrophilicity of the enzyme-bound FAD and the polarity of the active site (species 3 in Scheme 2) (*45*). Consistent with the proposed roles, the recent determination of the X-ray structure of choline oxidase showed that His_{466} is located ∼3.3 Å from the N(1) locus of the enzyme-bound flavin (Figure 1) (G. Lountos, F. Fan, G. Gadda, and A. M. Orville; unpublished results).

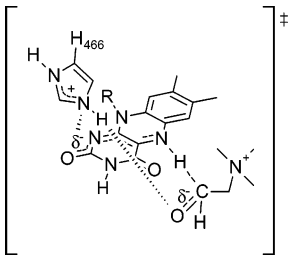

FIGURE 1: Line drawing showing the interaction of His_{466} with the N(1)−C(2)=O locus of FAD and the choline alkoxide species in the transition state for the oxidation of choline catalyzed by choline oxidase. The positioning of His_{466} relative to the flavin is from the X-ray crystallographic structure of the enzyme recently determined at 1.86 Å resolution (G. Lountos, F. Fan, G. Gadda, and A. M. Orville, unpublished results), and the positioning of choline is arbitrary.

In the study presented here, we have prepared by site-directed mutagenesis a choline oxidase variant in which His_{466} was replaced with aspartate and characterized the biochemical and biophysical properties of the enzyme-bound flavin in the mutant enzyme bearing a negative charge at position 466. The results presented show that the protein positive charge proximal to the flavin N(1) locus is important for correct flavinylation of the enzyme, modulation of flavin reactivity, and, consequently, the catalytic activity of the enzyme.

EXPERIMENTAL PROCEDURES

Materials. *Escherichia coli* strain Rosetta(DE3)pLysS was from Novagen (Madison, WI). The QuikChange site-directed mutagenesis kit was from Stratagene (La Jolla, CA). The

QIAprep Spin Miniprep kit was from Qiagen (Valencia, CA). Oligonucleotides used for site-directed mutagenesis and for sequencing of the mutant gene were custom synthesized by the DNA Core Facility of the Department of Biology of Georgia State University or by Sigma Genosys (The Woodlands, TX). Nucleotides, bovine serum albumin, chloramphenicol, tetracycline, isopropyl β-D-thiogalactopyranoside (IPTG), lysozyme, sodium hydrosulfite (dithionite), sodium sulfite, betaine aldehyde, glycine betaine, xanthine, xanthine oxidase, Luria-Bertani agar and broth, and PMSF were from Sigma (St. Louis, MO). Choline chloride and ampicillin were from ICN (Aurora, OH). Recombinant choline oxidase (CHO-WT)[1] from *Arthrobacter globiformis* strain ATCC 8010 was expressed in *E. coli* strain Rosetta(DE3)pLysS from plasmid pET/*codA*1 and purified to homogeneity as previously described (*38*). Fully oxidized FAD-containing CHO-WT was prepared as described in ref *44*. The mutant form of choline oxidase with histidine 466 replaced with alanine (CHO-H466A) was prepared, expressed, and purified to homogeneity according to the method of ref *45*. All other reagents were of the highest purity commercially available.

Instruments. UV−visible absorbance spectra were recorded using an Agilent Technologies model HP 8453 diode array spectrophotometer equipped with a thermostated water bath. Fluorescence spectra were recorded with a Shimadzu model RF-5301 PC spectrofluorometer thermostated at 15 °C. The enzymatic activity of choline oxidase was measured polarographically using a computer-interfaced Oxy-32 oxygen monitoring system (Hansatech Instrument Ltd.).

Site-Directed Mutagenesis. A QuikChange kit was used to prepare CHO-H466D, in which histidine 466 was replaced with aspartate. The method used was essentially according to the manufacturer's instructions, using the pET/*codA*1 plasmid (*38*) as a template and Cho-H466Df (5′-CAACACCGTCTACGACCCCGTGGGCACCGTGC-3′) and Cho-H466Dr (5′-CACGGTGCCCACGGGGTCGTAGACGGTGTTGTGC-3′) oligonucleotides as forward and reverse primers, respectively (underlined letters indicate mismatches). DNA was sequenced at the DNA Core Facility at Georgia State University using an Applied Biosystems Big Dye Kit on an Applied Biosystems model ABI 377 DNA sequencer. Sequencing confirmed the presence of the correct mutation. *E. coli* strain Rosetta(DE3)pLysS competent cells were transformed with plasmid pET/*codA*1-H466D by electroporation.

Expression and Purification of CHO-H466D. CHO-H466D was expressed and purified to homogeneity as judged by SDS−PAGE using the same procedure used previously for the purification of CHO-WT and CHO-H466A (*38*, *45*). Glycerol at a final concentration of 10% was incorporated in the buffers throughout the purification procedure to increase the stability of the enzyme.

Spectrophotometric Studies. The UV−visible absorbance and fluorescence emission or excitation spectra of CHO-H466D, CHO-WT, and CHO-H466A were acquired in 20 mM sodium phosphate, 20 mM sodium pyrophosphate, and 10% glycerol (pH 6) at 15 °C. The UV−visible absorbance spectra of the reduced form of enzymes were acquired using an anaerobic cuvette in 50 mM sodium phosphate, 50 mM sodium pyrophosphate, and 10% glycerol (pH 6) at 15 °C. The cuvette contained one ml final volume of enzyme at a final concentration between 20 and 30 μM, 300 μM xanthine, and 10 μM methyl viologen. A sidearm attached to the cuvette contained xanthine oxidase at a final concentration of ~0.5 μM. The cuvette and contents were made anaerobic by at least 15 cycles of alternate degassing under vacuum and flushing with O_2-free argon. The enzyme solution was then mixed with xanthine oxidase in the sidearm, and the reduction of the enzyme-bound flavin was monitored spectrophotometrically. Spectra of the reduced enzymes reported in this study were recorded prior to the accumulation of significant amounts of viologen radical.

The extinction coefficient of CHO-H466D was determined in 20 mM Tris-HCl (pH 8) after denaturation of the enzyme by incubation at 40 °C for 1 h in the presence of urea at a final concentration of 4 M, based upon the ϵ_{450} value of 11.3 mM^{-1} cm^{-1} for free FAD (*46*). A value of 12 mM^{-1} cm^{-1} was determined at 450 nm, which was similar to the values of 11.4 mM^{-1} cm^{-1} at 452 nm for CHO-WT and 12 mM^{-1} cm^{-1} at 458 nm for CHO-H466A (*40*, *45*). For the quantitation of covalently bound flavin, ~20 μM CHO-H466D was incubated on ice for 30 min after the addition of 10% trichloroacetic acid, followed by removal of precipitated protein by centrifugation. The concentration of FAD was then determined in both the supernatant and the pellet dissolved in a 4 M urea solution as described above. Identification of the flavin cofactor released by acid treatment was carried out through MALDI-TOF mass spectrometry in both positive and negative ion modes using a 50:50 methanol/acetonitrile matrix. Anaerobic incubation of CHO-H466D with choline was carried out in 20 mM Tris-HCl (pH 8) after anaerobiosis was established by repeated cycles of alternate degassing under vacuum and flushing with ultrapure O_2-free argon in an anaerobic cell equipped with two sidearms. Choline, at a final concentration of 10 mM, was initially loaded into a sidearm and subsequently mixed with CHO-H466D under anaerobiosis. A few grains of sodium dithionite were loaded into the second sidearm and mixed with CHO-H466D in complex with choline after 1 h of anaerobic incubation to ensure the functionality of the enzyme-bound flavin. Binding of glycine betaine and sulfite to the enzymes was carried out as previously described (*40*, *45*). The pH dependence of the UV−visible absorbance spectra of oxidized CHO-H466D was determined in 20 mM sodium phosphate, 20 mM sodium pyrophosphate, and 10% glycerol, at 15 °C, by titrating sodium hydroxide into the enzyme solution at pH 6. The pH dependences of the UV−visible absorbance spectra of the reduced enzymes were determined in a custom-made anaerobic cuvette (Lillie Glassblowers, Smyrna, GA) that was fitted with a pH microelectrode through a glass joint and an anaerobic syringe containing sodium hydroxide. The cuvette contained 3 mL of enzyme at a final concentration between 20 and 30 μM in 50 mM sodium phosphate, 50 mM sodium pyrophosphate, and 10% glycerol (pH 6). A sidearm attached to the cuvette was loaded with choline at a final concentration of 150 mM. The cuvette and contents were made anaerobic by at least 15 cycles of alternate

[1] Abbreviations: CHO-WT, wild-type choline oxidase; CHO-H466D, mutant form of choline oxidase with histidine 466 replaced with aspartate; CHO-H466A, mutant form of choline oxidase with histidine 466 replaced with alanine; E'_1 and E'_2, midpoint reduction−oxidation potential of the oxidized/semiquinone and semiquinone/reduced FAD redox couples, respectively; $E'_{m,7}$, midpoint reduction−oxidation potential of the oxidized/reduced FAD redox couple determined at pH 7.

degassing under vacuum and flushing with O_2-free argon. The enzyme solution was then mixed with choline in the sidearm to reduce the enzyme-bound flavin. With CHO-H466D, which could not be reduced anaerobically with choline, a syringe filled with anaerobic ~2 mM dithionite was inserted first into the cuvette under positive argon pressure, and the reduction of the enzyme-bound flavin was monitored spectrophotometrically until the process reached completion. In all the cases, once the UV−visible absorbance spectrum of the hydroquinone species was observed, a pH microelectrode and a syringe containing anaerobic 3 M sodium hydroxide were mounted onto the anaerobic cuvette under positive argon pressure. The pH of the anaerobic enzyme solution was then changed stepwise by addition of the base, and both the pH and the UV−visible absorbance spectra were recorded after each step.

Potentiometric Titrations. The midpoint reduction−oxidation potentials of unliganded CHO-H466D, CHO-H466A, and CHO-WT were determined through the reductive titration of the enzyme with sodium dithionite as a reductant as previously described for CHO-WT and CHO-H466A in complex with glycine betaine (*45*).

Enzyme Assays. The enzymatic activity of CHO-H466D was measured polarographically with choline by measuring the rate of oxygen consumption as described for the wild-type enzyme (*38*, *40*).

Data Analysis. Data of the spectrophotometric titrations for formation of a complex of choline oxidase and various ligands were fit to eq 1

$$Y = \frac{AX}{X + K} \quad (1)$$

where Y and A are the observed and maximal absorbance changes at the selected wavelength, respectively, X is the concentration of the varied ligand, and K is the complex dissociation constant. Data of the pH dependencies of the absorbance spectra were fit to eq 2, which describes a curve with a slope of 1 and plateau regions at low and high pH

$$Y = (A \times 10^{-pK_a} + B \times 10^{-pH})/(10^{-pH} + 10^{-pK_a}) \quad (2)$$

where A and B represent the absorbance values at 500 nm at low and high pH, respectively. The midpoint reduction−oxidation potentials of the enzymes were determined by fitting the data to eq 3

$$E_h = E'_m + (2.303RT/nF) \log\frac{[FAD_{ox\ or\ sq}]}{[FAD_{sq\ or\ red}]} \quad (3)$$

where E_h is the observed electrode potential at equilibrium at each point in the titration, E'_m is the midpoint reduction−oxidation potential, R is the gas constant, with a value of 8.31 J mol^{-1} K^{-1}, T is the temperature in kelvin, n is the number of electrons transferred, and F is Faraday's constant, with a value of 96.48 kJ V^{-1} mol^{-1}.

RESULTS

Expression and Purification of CHO-H466D. CHO-H466D was expressed and purified at pH 8 to a high level as judged by SDS−PAGE using the same protocol used for the wild-type enzyme (Figure S1 of the Supporting Information). Approximately 100−150 mg of pure CHO-H466D could be typically obtained from 4.5 L of Luria-Bertani culture medium. In contrast to the wild-type enzyme, for which 35−85% of the bound flavin exists at pH 8 in an air-stable anionic semiquinone state (*38*, *40*) that can be oxidized by extended incubation at pH 6 (*40*), the flavin in CHO-H466D was in the oxidized state throughout the purification procedure. In this respect, CHO-H466D is similar to CHO-H466A, for which no flavin semiquinone was observed in the UV−visible absorbance spectrum of the purified enzyme (*45*). Purified CHO-H466D at final concentrations as high as 20 μM showed no oxygen consumption when assayed with 30 mM choline as a substrate at pH 7 and 25 °C. In comparison, CHO-WT at a final concentration of 0.1 μM typically shows a catalytic activity of ~15 s^{-1} with 10 mM choline (*38*), suggesting that replacement of the histidine at position 466 with aspartate results in the complete loss of catalytic activity in choline oxidase.

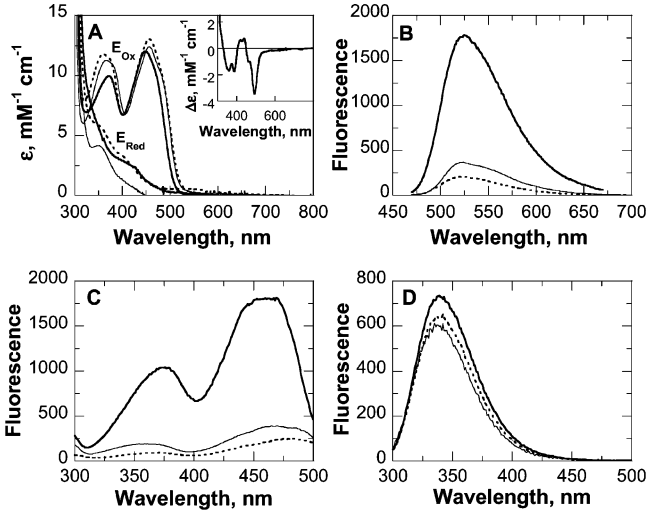

FIGURE 2: Comparison of the spectral properties of CHO-H466D (thick solid curves), CHO-WT (thin solid curves), and CHO-H466A (dotted curves) in 20 mM sodium phosphate, 20 mM sodium pyrophosphate, and 10% glycerol at pH 6 and 15 °C. (A) UV−visible absorbance spectra of the oxidized and reduced species of enzymes after treatment with xanthine (300 μM) and xanthine oxidase (~0.5 μM). The inset shows the difference absorbance spectrum of oxidized CHO-H466D (thick solid curve) minus that of CHO-WT as a reference. (B) Flavin fluorescence emission spectra for which the excitation wavelengths were 447, 457, and 457 nm for CHO-H466D, CHO-WT, and CHO-H466A, respectively. (C) Flavin fluorescence excitation spectra for which the emission wavelength was 530 nm for all forms of the enzyme. (D) Protein fluorescence emission spectra for which the excitation wavelengths were 285 nm.

Spectral Properties of Oxidized CHO-H466D. The UV−visible absorbance spectrum of oxidized CHO-H466D at pH 6[2] showed a 10 nm hypsochromic shift of the visible peak centered at ~450 nm and a 10% decrease in the intensity of the 372 nm peak with respect to those of both CHO-WT and CHO-H466A (Figure 2A), suggesting an altered protein

[2] The spectral properties of the oxidized forms of CHO-WT, CHO-H466A, and CHO-H466D were compared at pH 6 to prevent artifactual contributions to the UV−visible absorbance spectra due to pH, since the three enzyme variants exhibited pH effects on the UV−visible absorbance spectra of the oxidized enzymes with a pK_a of ≥8.2 (this study and ref *45*).

Table 1: Comparison of the Spectral Parameters of CHO-H466D, CHO-H466A, and CHO-WT at pH 6

	CHO-H466D	CHO-H466A	CHO-WT
	E−FAD_{Ox}		
UV−visible absorbance (λ_{max}, nm)	276, 372, 447	267, 361, 457	279, 366, 457
ϵ (mM^{-1} cm^{-1})	210, 10, 12	272, 11.8, 13	154, 11.3, 12.4
stoichiometry (no. of FAD/protein)	0.29 ± 0.03	0.32 ± 0.05[a]	0.88 ± 0.12[b]
% of FAD covalently bound	∼25	100[a]	100[b]
fluorescence emission (λ_{max}, nm)			
λ_{ex} = 447 or 457 nm	525	524	524
λ_{ex} = 372, 361, or 366 nm	524	519	522
λ_{ex} = 285 nm	339	342	335
fluorescence excitation (λ_{max}, nm)			
λ_{em} = 530 nm	376, 460	371, 475	361, 470
pK_a[N(3)−H]	10.3 ± 0.1	9.3 ± 0.2[a]	8.2 ± 0.1[a]
	E−FAD_{Red}		
UV−visible absorbance (λ_{max}, nm)	∼340, ∼400	∼350, ∼400	347
ϵ (mM^{-1} cm^{-1})	∼6.7, ∼2.9	∼5.8, ∼3.3	4.2
	E−FAD_{Ox}−glycine betaine		
UV−visible absorbance (λ_{max}, nm)	nd[c]	361, 459	358, 455
K_d (mM)	nd[c]	4.2 ± 0.4	15 ± 2
K_{is}[d] (mM)	nd[c]	5.2 ± 0.5	13 ± 1

[a] From ref *45*. [b] From ref *38*. [c] Not determined. [d] Limiting inhibition constant determined kinetically with choline as the substrate at low pH; from ref *45*.

microenvironment in the protein containing aspartate at position 466. Accordingly, the relative intensity of the flavin fluorescence emission at ∼525 nm (with λ_{ex} at 447 nm) was 5 and 10 times larger than that observed with CHO-WT and CHO-H466A, respectively (Figure 2B). Similarly, the flavin fluorescence excitation spectrum of CHO-H466D had maxima at 376 and 460 nm (with λ_{em} at 530 nm), with intensities 5- and 10-fold greater than those seen with CHO-WT and CHO-H466A, respectively (Figure 2C). In contrast, no significant differences were seen in the intensities of the protein fluorescence emission peaks at 340 nm among the three different forms of enzyme (Figure 2D), suggesting that the overall folds of the mutant enzymes were similar to that of the wild-type enzyme. The spectral properties of oxidized CHO-H466D, CHO-WT, and CHO-H466A are summarized in Table 1.

Flavin Stoichiometry and Content of CHO-H466D. Previous studies showed that choline oxidase contains covalently linked FAD in a 1:1 stoichiometry (*38*). In contrast, upon denaturation of the CHO-H466D variant by treatment with urea, a stoichiometry of 0.29 ± 0.03 FAD per monomer of enzyme could be determined from two independent experiments. Similar flavin content was previously reported for the CHO-H466A variant (Table 1) (*45*), suggesting that the flavin content in choline oxidase is significantly affected by replacement of the active site histidine with either a neutral or an anionic amino acid residue. Interestingly, treatment of CHO-H466D with 10% cold trichloroacetic acid followed by centrifugation to remove the denatured protein yielded a UV−visible absorbance spectrum of the soluble fraction with peaks at 370 and 450 nm, suggesting that at least part of the flavin in CHO-H466D is not covalently bound (Figure S2 of the Supporting Information). A MALDI-TOF mass spectrometric analysis of the flavin released from CHO-H466D yielded a *m*/*z* ratio of 784.1 (Figure S2 of the Supporting Information), consistent with the noncovalently bound flavin in CHO-H466D being FAD. From the intensities of the peaks at 450 nm in the supernatant and pellet dissolved in 4 M urea obtained upon acid treatment of CHO-H466D, it was estimated that ∼75% of the flavin in CHO-H466D is tightly but not covalently bound to the enzyme. These data clearly suggest that reversing the positive charge in the proximity of the FAD N(1) locus affects not only the flavin content in the protein but also the extent of protein flavinylation.

Spectrophotometric Properties of Reduced CHO-H466D. The UV−visible absorbance spectrum of the fully reduced form of CHO-H466D was obtained by anaerobic incubation of the enzyme with xanthine and xanthine oxidase, at pH 6. As shown in Figure 2A, an indistinct shoulder with no well-defined peaks was observed in the 400−450 nm region of the absorbance spectrum of CHO-H466D hydroquinone, suggesting that at pH 6 the flavin hydroquinone bound to this enzyme variant was present in the neutral form (*47*−*49*). During the reduction process, no flavin semiquinone intermediate was observed (data not shown). A similar reduction of CHO-WT yielded a UV−visible absorbance spectrum with a well-defined peak at 347 nm (Figure 2A), consistent with previous data on anaerobic substrate reduction of the wild-type enzyme that suggested the presence of the reduced flavin in the anionic state (*40*). In the case of CHO-H466A, anaerobic reduction of the enzyme at pH 6 resulted in a UV−visible absorbance spectrum with features that were intermediate between those of CHO-H466D and CHO-WT, i.e., both a poorly defined peak at ∼350 nm and a shoulder in the 400 nm region (Figure 2A). Thus, at pH 6 the reduced flavin in CHO-H466A is likely present as a mixture of anionic and neutral hydroquinones. The spectral properties of the three enzyme variants in the reduced state are summarized in Table 1.

Effect of pH on the Spectrophotometric Properties of CHO-H466D. The effects of pH on the UV−visible absorbance spectra of CHO-H466D were determined on the oxidized and reduced enzymes. As shown in Figure 3, the absorbance at 500 nm increased between limiting values with an increase in pH, yielding a pK_a value of 10.3 ± 0.1, which could be assigned to the ionization of the N(3) locus of the oxidized enzyme-bound FAD (*50*). Previous data on CHO-H466A and CHO-WT yielded pK_a values of ∼9.3 and ∼8.2, respectively (*45*), consistent with significant changes in the

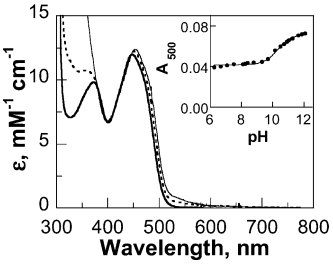

FIGURE 3: Effect of pH on the spectral properties of CHO-H466D. UV−visible absorbance spectra were recorded at an enzyme concentration of ~20 μM in 20 mM sodium phosphate, 20 mM sodium pyrophosphate, and 10% glycerol at 15 °C. Only selected spectra are shown for the enzyme at pH 6 (thick solid curve), pH 10 (dotted curve), and pH 12 (thin solid curve). The inset shows the absorbance values at 500 nm as a function of pH; data were fit to eq 2.

microenvironment surrounding the FAD N(3) locus upon replacement of His_{466} with a neutral or anionic amino acid.

No significant spectral changes were observed in the UV−visible absorbance spectrum of CHO-H466D hydroquinone when the pH was increased from 6 to 10, consistent with the neutral species of the reduced flavin being stabilized in this pH range (data not shown). Similarly, no spectral changes were observed in the same pH range with CHO-WT hydroquinone, suggesting that ionization of the N(1) position of FAD has a pK_a significantly lower than 6 or that the N(1) position of FAD is not solvent accessible in the wild-type reduced enzyme (data not shown). In contrast, the UV−visible absorbance spectrum of CHO-H466A hydroquinone at pH 8 exhibited features that are typically associated with the anionic reduced flavin, i.e., a distinct peak at 356 nm (Figure S3 of the Supporting Information). Thus, in CHO-H466A, the relative amount of anionic versus neutral hydroquinone increased significantly when the pH was increased from 6 to 8, suggesting that the flavin N(1) locus in this enzyme variant is both solvent accessible and ionizable in this pH range.

Redox Potentiometry of Unliganded CHO-H466D, CHO-H466A, and CHO-WT. Previous studies established that with choline oxidase in complex with glycine betaine the replacement of His_{466} with alanine resulted in a decrease of the midpoint reduction−oxidation potential for the oxidized−reduced flavin couple from 132 to 106 mV at pH 7 (*45*). Since CHO-H466D does not bind glycine betaine but forms a stable complex without reacting with choline (vide infra), here we have attempted to determine the reduction−oxidation potential of CHO-H466D in the presence of 10 mM choline at pH 7 and 15 °C. However, significant turbidity of the enzyme solution developed during the course of the reduction (Figure S4 of the Supporting Information), preventing the determination of the reduction−oxidation potential of CHO-H466D in complex with a ligand. Consequently, the midpoint reduction−oxidation potential of CHO-H466D, and those for CHO-WT and CHO-H466A for comparison, were determined on the free enzymes in the absence of ligands at pH 7. With both CHO-WT and CHO-H466A, the midpoint reduction−oxidation potentials for the first and second reducing equivalents were well-separated, resulting in the thermodynamic stabilization of the flavin anionic semiquinone species (Figure 4A−D). In agreement with the observed potentials for the first and second electron transfer

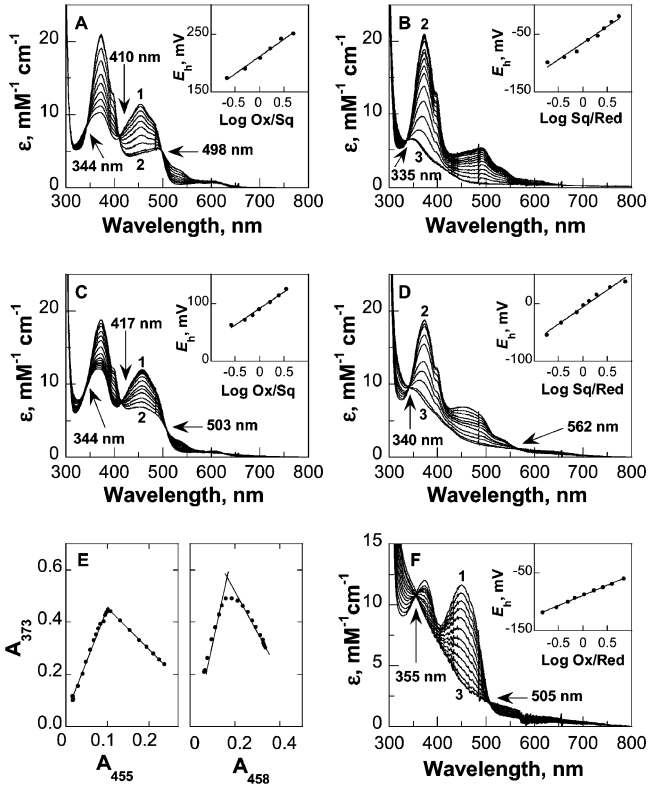

FIGURE 4: Potentiometric reduction−oxidation titration of CHO-WT (A and B), CHO-H466A (C and D), and CHO-H466D (F) at concentrations of ~20 μM in 20 mM Tris-HCl at pH 7 and 15 °C: curve 1, UV−visible absorbance spectra of the oxidized species of enzymes; curve 2, UV−visible absorbance spectra of the maximum red anionic semiquinone that formed during the reductive titrations; and curve 3, UV−visible absorbance spectra of the fully reduced species of enzymes. (E) Quantitation of the amount of flavin semiquinone formed with CHO-WT (left) and CHO-H466A (right). Insets show the determination of the midpoint reduction potentials: (A−D) Nernst plots of the potentiometric data for the reduction of the enzyme-bound flavin in CHO-WT and CHO-H466A (A and C, Ox → Sq; B and D, Sq → Red) for which data were fit to eq 3 and (F) Nernst plot of the potentiometric data for the reduction of the enzyme-bound flavin in CHO-H466D (Ox → Red) for which data were fit to eq 3.

equilibria, 100 and 90% of flavin semiquinones were seen with CHO-WT and CHO-H466A, respectively (Figure 4E and Table 2). In contrast, with CHO-H466D, no flavin semiquinone was observed during reduction of the enzyme at pH 7, resulting in the determination of the $E'_{m,7}$ values for the oxidized−reduced enzyme couple (Figure 4F). In all cases, the analyses of the data according to the Nernst formalism yielded lines in plots of E_h versus log([oxidized or semiquinone species]/[semiquinone or reduced species]) with slopes of ~59 and 35 for the one- and two-electron transfers, respectively, in agreement with the expected values of 57 and 28.5 mV, respectively, at 15 °C (Figure 4 and Table 2). As illustrated in Table 2, the $E'_{m,7}$ for the transfer of the two electrons with CHO-H466D had a value that was ~130 and ~160 mV more negative than the calculated midpoint potentials for the corresponding two-electron transfers in CHO-H466A and CHO-WT, respectively. These data are consistent with a significant effect of the amino acid residue at position 466 on the electrophilicity of the enzyme-bound flavin in choline oxidase. Interestingly, the midpoint reduction−oxidation potential for the oxidized−semiquinone couple in wild-type choline oxidase was 211 mV, which is

Table 2: Midpoint Reduction−Oxidation Potentials for the Enzyme−FAD Forms of Unliganded CHO-WT, CHO-H466A, and CHO-H466D at pH 7[a]

enzyme	E'_1 (mV)[b] [slope (mV)]	E'_2 (mV)[c] [slope (mV)]	% Sq	$E'_{m,7}$ (mV)[d] [slope (mV)]
CHO-WT	211 ± 2 [60 ± 3]	−65 ± 2 [57 ± 4]	100	73[e]
CHO-H466A	91 ± 2 [57 ± 3]	−6 ± 2 [59 ± 3]	90	42.5[e]
CHO-H466D	na[f]	na[f]	0	−89 ± 1 [35 ± 1]

[a] Conducted in 20 mM Tris-HCl at pH 7 and 15 °C. [b] Midpoint potential ($n = 1$) of the oxidized/semiquinone FAD redox couple. [c] Midpoint potential ($n = 1$) of the semiquinone/hydroquinone FAD redox couple. [d] Midpoint potential ($n = 2$) of the oxidized/hydroquinone FAD redox couple. [e] Calculated midpoint potential for CHO-WT and CHO-H466A [$E'_{m,7} = (E'_1 + E'_2)/2$ (*64*)]. [f] Not available.

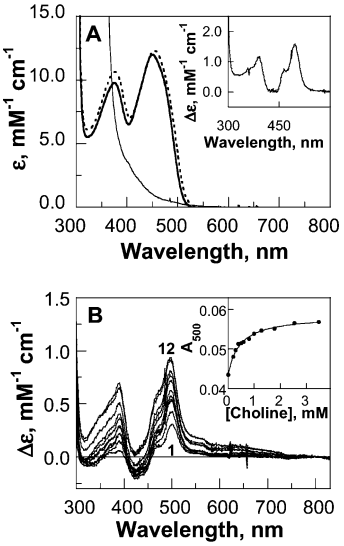

FIGURE 5: Binding of choline to CHO-H466D. (A) UV−visible absorbance spectra of CHO-H466D were recorded at a concentration of ~30 μM in 20 mM Tris-HCl at pH 8 and 15 °C, before modification (thick solid curve), after anaerobic incubation of the enzyme with 10 mM choline for 1 h (dotted curve), and after the addition of dithionite powder (thin solid curve). The inset shows the difference spectrum of the enzyme bound to the free enzyme. (B) Difference absorbance spectra of CHO-H466D at a concentration of ~20 μM in 20 mM Tris-HCl at pH 8 and 15 °C, during the aerobic titration of choline in the concentration range between zero (curve 1) and 3.5 mM (curve 12). The inset shows the absorbance values at 500 nm as a function of choline concentration; data were fit to eq 1.

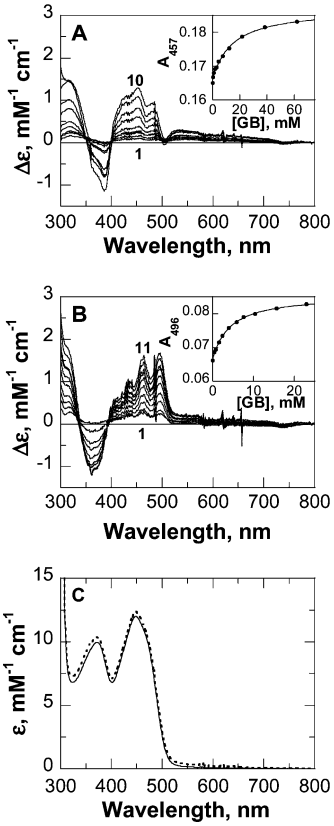

FIGURE 6: Binding of glycine betaine to CHO-WT, CHO-H466A, and CHO-H466D. Difference spectra of CHO-WT (A) and CHO-H466A (B) during the aerobic titration of glycine betaine in a concentration range between zero (curve 1 in panels A and B) and 62 mM (curve 10 in panel A) or 23 mM (curve 11 in panel B). Insets show absorbance values at 457 nm (A) and 496 nm (B) as a function of glycine betaine concentration for CHO-WT and CHO-H466A; the curves are fits of the data to eq 1. (C) UV−visible absorbance spectra of CHO-H466D before (solid curve) and after aerobic titration of glycine betaine up to a final concentration of ~80 mM (dotted curve). Absorbance spectra were recorded at an enzyme concentration of ~20 μM in 20 mM sodium phosphate, 20 mM sodium pyrophosphate, and 10% glycerol at pH 6.

to our knowledge the highest value for such thermodynamic equilibrium reported for a flavoprotein oxidase (*9*, *11*, *51*−*56*).

Binding of Choline, Glycine Betaine, and Sulfite to CHO-H466D. In agreement with the lack of oxygen consumption of CHO-H466D when it is assayed polarographically with choline as the substrate, the anaerobic mixing of this mutant protein with 10 mM choline resulted in no bleaching of the flavin peak at ~450 nm over an incubation period of 60 min, as shown in Figure 5A. However, a 4 nm batochromic shift associated with an increase in absorbance at 375 nm was observed in the UV−visible absorbance spectrum of CHO-H466D in the presence of choline (Figure 5A). These spectral changes were similar to those seen for the CHO-H466A variant in a complex with glycine betaine (Figure 6B), suggesting that CHO-H466D retained the ability to bind choline at the active site without subsequent oxidation of the substrate. The lack of reactivity of CHO-H466D with choline was exploited for the determination of an equilibrium constant for the dissociation of choline from the enzyme (K_d) of 0.45 ± 0.04 mM at pH 8, a process which was carried out spectrophotometrically by following the UV−visible spectral changes of the enzyme in the visible region at increasing concentrations of choline (Figure 5B). Such a K_d value was 4 times lower than the K_d value of ~1.8 mM that was recently determined through rapid reaction studies of CHO-WT reacting with choline at pH 8 (*57*), suggesting that reversing the charge at position 466 results in a slightly tighter binding of choline to the active site of the enzyme.

The lack of enzymatic activity of CHO-H466D prevented a kinetic determination of the inhibition constant for binding of glycine betaine to the enzyme, which was previously carried out for both CHO-WT (*40*) and CHO-H466A (*45*). Consequently, the determination of the dissociation constant

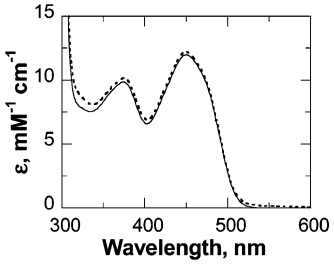

FIGURE 7: Reaction of CHO-H466D with sulfite. UV−visible absorbance spectra of CHO-H466D before (solid curve) and after aerobic incubation with 100 mM sodium sulfite for 3 h (dotted curve). The enzyme concentration was 15 μM in 100 mM sodium pyrophosphate at pH 6 and 15 °C.

for glycine betaine binding was carried out with the wild-type and mutant forms of choline oxidase by following the spectral changes associated with mixing of the enzyme with increasing ligand concentrations. With both CHO-WT and CHO-H466A, K_d values for glycine betaine binding that were in good agreement with those previously determined using the kinetic approach could be determined at pH 6 (Figure 6A,B and Table 1) (*40*, *45*). In contrast, no significant spectral changes could be observed with CHO-H466D at concentrations of glycine betaine as high as 80 mM (Figure 6C), suggesting that choline oxidase lost the ability to bind glycine betaine when the active site histidine was replaced with aspartate.

Wild-type choline oxidase was shown previously to form a tight reversible N(5) flavin−sulfite adduct with a K_d value of ~50 μM at pH 7 and 15 °C (*40*). In contrast, with CHO-H466A, an N(5) flavin−sulfite adduct could be obtained only in the presence of exogenous imidazole, while in the absence of imidazole, no adduct could be formed even after incubation of CHO-H466A with 100 mM sulfite for 3.5 h (*45*). Similarly, no spectral changes could be detected here when CHO-H466D was incubated for 3 h at pH 6 and 15 °C in the presence of 100 mM sodium sulfite (Figure 7), consistent with lack of stabilization of the sulfite−flavin adduct in CHO-H466D.

DISCUSSION

A recent biochemical and mechanistic study of a mutant form of choline oxidase in which the active site histidine at position 466 was replaced with alanine established the involvement of His_{466} in the reductive half-reaction in which choline is oxidized to betaine aldehyde, but not in the following oxidative half-reaction in which oxygen is reduced to hydrogen peroxide (*45*). Of particular interest was the finding that in catalysis His_{466} is protonated, as suggested by the observation that the enzymatic activity of CHO-H466A could be partially rescued in the presence of exogenous imidazolium, but not imidazole (*45*). The positively charged His_{466} was proposed to play multiple roles in the oxidation of choline catalyzed by choline oxidase, by contributing to the polarity of the active site, stabilizing the negatively charged transition state, and activating the flavin for the oxidation reaction (*45*). As illustrated in Scheme 2, the contribution of His_{466} to the active site polarity would be required for the efficient removal of the substrate hydroxyl proton that results in the activation of the substrate (species 1 and 2). The stabilization of the resulting choline alkoxide species (species 2) and the activation of the enzyme-bound flavin (species 3) would correctly position and facilitate the quantum mechanical transfer of the hydride from the substrate α-carbon to the N(5) flavin locus (species 3) (*39*, *41*, *45*). The recent determination of the crystal structure of choline oxidase showed that His_{466} is located in the active site ~3.3 Å from the N(1) locus of the flavin (Figure 1) (G. Lountos, F. Fan, G. Gadda, and A. M. Orville, unpublished results), consistent with the proposed roles for this residue in catalysis. In the study presented here, we have prepared a second variant of choline oxidase in which His_{466} was replaced with an aspartate residue by site-directed mutagenesis and investigated the effects of reversing the charge in the proximity of the N(1) locus of the flavin by using biochemical and biophysical approaches.

From a biophysical standpoint, reversing the protein positive charge at position 466 in choline oxidase results in the lack of stabilization of the negative charge that is produced on the N(1) locus of the enzyme-bound flavin in the one- and two-electron-reduced forms of choline oxidase. Evidence for this conclusion comes primarily from the UV−visible absorbance spectrum of the two-electron-reduced form of CHO-H466D at pH 6, which is consistent with the enzyme-bound flavin hydroquinone being in the neutral state (*47*−*49*). The lack of changes in the UV−visible absorbance spectrum of the reduced flavin when the pH is increased from 6 to 10 is further consistent with stabilization of the neutral flavin hydroquinone in CHO-H466D being due to the effect of the negatively charged aspartyl side chain, since such a residue is expected not to change its ionization state above pH 6. In contrast, the wild-type enzyme stabilizes the anionic form of hydroquinone between pH 6 and 10, as shown by the well-resolved peak at 356 nm in the UV−visible absorbance spectrum of the two-electron-reduced enzyme. These data, in turn, suggest that the histidyl side chain at position 466 either decreases the pK_a value for the ionization of the N(1) FAD locus in the reduced enzyme to values of <6 or hinders solvent accessibility to the N(1) locus, thereby preventing its protonation during flavin reduction. In agreement with these conclusions, the alanyl variant of the enzyme, which carries a small and neutral side chain proximal to the FAD N(1) position, exists as a mixture of neutral and anionic hydroquinones at pH 6 and as the anionic species at pH 8. The different stabilization of the negative charge on the N(1) locus of the flavin in the hystidyl, alanyl, and aspartyl enzymes is independently suggested by the observation that the anionic flavin semiquinone was stabilized at pH 7 in only the wild-type and H466A mutant enzymes, but not in CHO-H466D. These results suggest that at least in choline oxidase the removal of the positive charge in the proximity of the N(1) locus of the flavin is not sufficient to destabilize the anionic flavin semiquinone and that such a destabilization requires the presence of a protein negative charge. Finally, the lack of changes in the UV−visible absorbance spectrum of oxidized CHO-H466D in the presence of sodium sulfite, which was previously observed to form a tight reversible N(5) flavin adduct with the wild-type enzyme (*40*), provides independent evidence that replacing the protein positive charge at position 466 results in a lack of stabilization of the negative charge on the N(1)−C(2)═O flavin locus.

The most dramatic effect arising from the lack of stabilization of the negative charge on the pyrimidine ring of the

reduced flavin in CHO-H466D is that ~75% of the enzyme-bound FAD is tightly, but not covalently, bound to the protein moiety. This conclusion is supported by the analysis of the supernatant obtained upon acid treatment of the enzyme containing aspartate at position 466 followed by centrifugation to remove the denatured protein. In contrast, both CHO-WT and CHO-H466A have recently been reported to contain only covalently bound FAD (*38*, *45*), suggesting that replacing the protein positive charge close to the N(1) atom of the flavin with a neutral residue is not sufficient to affect the flavinylation of the enzyme. With both the aspartyl and alanyl mutant proteins, the total FAD content was 3−4-fold lower than that previously observed for the wild-type enzyme, in which a 1:1 stoichiometry of FAD to protein was established, further suggesting that the presence of a protein positive charge close to the N(1) position of the flavin is important for the formation of the covalent linkage between FAD and the protein in choline oxidase. These results are in keeping with other studies recently reported on trimethylamine dehydrogenase, sarcosine oxidase, *N*-methyltryptophan oxidase, and *p*-cresol methylhydroxylase (*20*, *58*−*61*), suggesting that a positively charged microenvironment close to the flavin N(1)−C(2)═O locus is important for the stabilization of negatively charged reduced flavin that is proposed to transiently form during the covalent attachment of the flavin to either the 6- or 8-position of the isoalloxazine ring (*61*).

From a functional standpoint, the most notable effect of reversing the protein positive charge on the side chain at position 466 in choline oxidase is an ~160 mV decrease in the midpoint reduction−oxidation potential of the enzyme-bound flavin for the two-electron transfer occurring between the oxidized and reduced enzyme-bound flavin. Such an effect arises from both the lack of covalent linkage between the enzyme-bound flavin and the protein and the presence of the negatively charged aspartyl side chain near the flavin N(1) locus. Earlier results on a number of flavin-dependent enzymes containing covalently bound flavins, namely, cholesterol oxidase (*62*), vanillyl-alcohol oxidase (*55*), and *p*-cresol methylhydroxylase (*54*), showed that, irrespective of the type of flavin linkage and protein, removing the covalent linkage between the flavin and the enzyme results in a decrease in the $E'_{m,7}$ value of the bound flavin of ~100 mV. If one assumes a similar contribution to the $E'_{m,7}$ value of ~100 mV from the covalent linkage in choline oxidase, the effect of the negative charge of the aspartyl side chain on the midpoint reduction−oxidation potential of the flavin in CHO-H466D can be estimated to be −60 mV. Since a 30 mV decrease in the $E'_{m,7}$ value was observed in this study upon replacement of His_{466} with alanine, it can be concluded that the electrophilicity of the enzyme-bound flavin is increased by ~6 kJ/mol in the presence of a positive charge and decreased by a similar extent in the presence of a negative charge near the N(1) locus of the flavin. A similar energetic contribution of a protein positive charge near the flavin N(1) locus on the electrophilicity of the flavin was previously reported for lactate monooxygenase, in which substituting Lys_{266} with a methionine residue resulted in a decrease of 30 mV in the midpoint reduction−oxidation potential of the flavin (*35*). Although replacement of a histidine with either an aspartate or glutamate residue was previously reported in cholesterol oxidase from *B. sterolicum*, no potentiometric data were reported in that study (*63*). Consequently, this is the first instance in which the effect of reversing the charge near the flavin N(1) locus on the electrophilicity of the enzyme-bound flavin has been investigated in a flavin-dependent oxidase.

Reversing the positive charge of His_{466} with aspartate in choline oxidase results in the complete loss of enzymatic activity, as suggested by the lack of both oxygen consumption and bleaching of the enzyme-bound flavin upon mixing of CHO-H466D with choline. The loss of enzymatic activity correlates well with the $\Delta E'_{m,7}$ value of ~160 mV observed between CHO-H466D and CHO-WT, which accounts for an ~250000-fold decrease in the rate of hydride transfer to the flavin in the H466D mutant enzyme as compared to that in the wild-type enzyme.[3] However, the 30 mV decrease in the $E'_{m,7}$ value observed here for CHO-H466A, which agrees with the previously reported value of ~25 mV (*45*), cannot fully explain the 20-fold decrease in the rate of choline oxidation that was previously reported for CHO-H466A compared to that of the wild-type enzyme (*45*). With CHO-H466A, the decrease in catalytic activity was explained by both a decrease in the flavin electrophilicity, which is reflected in the $E'_{m,7}$ value, and the lack of stabilization of the negatively charged alkoxide species that is transiently formed in the oxidation of choline (*45*). The data presented here with CHO-H466D, which could not bind glycine betaine or sulfite, suggest that the H466D variant likely also lost the ability to stabilize extra negative charges in the active site.[4] Similar results in which the enzyme did not show catalytic activity upon replacement of the protein positive charge near the flavin N(1) locus were previously reported for active site mutant forms of cholesterol oxidase in which His_{447}, which is the residue equivalent to His_{466} of choline oxidase, was replaced with either a glutamate or aspartate residue. However, in that study, the characterization of the enzyme-bound flavin was not reported.

Our recent study on the H466A mutant protein of choline oxidase showed that the enzymatic activity of the enzyme is only 20 times lower than that of the wild-type enzyme and that, most importantly, the enzymatic activity could be partially rescued in the presence of exogenous imidazolium but not imidazole in the assay reaction mixture (*45*). Although these data are consistent with H_{466} acting as an electrostatic catalyst by stabilizing the transient alkoxide species that forms in the oxidation of choline (species 2 and 3 in Scheme 2), they do not unequivocally rule out His_{466} being the general base catalyst that removes the hydroxyl proton of the substrate (species 1 in Scheme 2). Indeed, His_{466}

[3] A more rigorous approach for the correlation of the loss of enzymatic activity of CHO-H466D with the change in the midpoint oxidation−reduction potential of the enzyme-bound flavin would entail a study of the linear free energy relationship of the rate of flavin reduction using choline oxidase reconstituted with a number of flavin analogues. Such an analysis was beyond the scope of this study.

[4] The denaturation of the enzyme that ensues upon anaerobic reduction of CHO-H466D in complex with saturating concentrations of choline is also consistent with the inability of CHO-H466D to accommodate an extra negative charge in the active site. Indeed, while the anaerobic reduction of the free unliganded enzyme results in the stabilization of the neutral hydroquinone, it is likely that the presence of choline in the active site hinders solvent access to the N(1) position of the bound flavin, thereby preventing its protonation during reduction with the consequent unfolding of the protein due to charge repulsion between Asp_{466} and the negatively charged reduced flavin.

would still be able to electrostatically stabilize the anionic species of the substrate after removing the hydroxyl proton from the substrate and acquiring a positive charge. If this were the case, substitution of His_{466} with aspartate would be expected to generate a mutant enzyme with at least partial catalytic activity, since the negatively charged aspartyl side chain at position 466 would be neutralized upon abstraction of the substrate hydroxyl proton, thereby allowing the transient formation of the alkoxide species. However, the observation that CHO-H466D is completely devoid of enzymatic activity with choline is not consistent with Asp_{466} acting as a base in the active site of the aspartyl mutant of choline oxidase.

In summary, the results of the biochemical and biophysical investigation of a choline oxidase variant in which the protein charge near the flavin N(1) locus was reversed by site-directed mutagenesis suggest that the enzyme has lost the ability to stabilize negative charges in the active site, irrespective of whether they develop on the flavin or are borne on active site ligands. This effect results in the defective flavinylation of the protein, the decreased electrophilicity of the enzyme-bound flavin, and, consequently, the loss of catalytic activity in the enzyme. The latter conclusion is further consistent with His_{466} in the wild-type enzyme not acting as a general base catalyst in the reductive half-reaction in which choline is initially activated to the alkoxide species upon removal of its hydroxyl proton. Taken together, the data presented here provide further evidence of the importance of a protein positive charge close to the N(1) flavin in choline oxidase and, by extension, in flavoprotein oxidases and indicate that the enzyme loses its functionality upon reversal, but not neutralization, of such a positive charge.

ACKNOWLEDGMENT

This paper is dedicated to the memory of the late Professor Vincent Massey (1927−2002). We thank Ms. Kunchala Rungsrisuriyachai for kindly providing purified wild-type choline oxidase for the potentiometric experiments and Dr. Siming Wang for the MALDI-TOF mass spectrometric analysis of the flavin extracted from CHO-H466D.

SUPPORTING INFORMATION AVAILABLE

SDS−PAGE slab illustrating the purification of CHO-H466D (Figure S1), spectrophotochemical and MALDI-TOF mass spectroscopic analyses for the determination of the stoichiometry and flavin content of CHO-H466D (Figure S2), anaerobic reduction of CHO-H466A with xanthine and xanthine oxidase at pH 8 (Figure S3), and the attempted determination of the midpoint reduction−oxidation potential of CHO-H466D in a complex with choline (Figure S4). This material is available free of charge via the Internet at http://pubs.acs.org.

REFERENCES

1. Massey, V., Ghisla, S., and Moore, E. G. (1979) 8-Mercaptoflavins as active site probes of flavoenzymes, *J. Biol. Chem. 254*, 9640−50.
2. Fitzpatrick, P. F., and Massey, V. (1983) The reaction of 8-mercaptoflavins and flavoproteins with sulfite. Evidence for the role of an active site arginine in D-amino acid oxidase, *J. Biol. Chem. 258*, 9700−5.
3. Massey, V., Müller, F., Feldberg, R., Schuman, M., Sullivan, P. A., Howell, L. G., Mayhew, S. G., Matthews, R. G., and Foust, G. P. (1969) The reactivity of flavoproteins with sulfite. Possible relevance to the problem of oxygen reactivity, *J. Biol. Chem. 244*, 3999−4006.
4. Müller, F. (1972) On the interaction of flavins with phosphine-derivatives, *Z. Naturforsch., B 27*, 1023−6.
5. Massey, V., and Hemmerich, P. (1980) Active-site probes of flavoproteins, *Biochem. Soc. Trans. 8*, 246−57.
6. Macheroux, P., Kieweg, V., Massey, V., Soderlind, E., Stenberg, K., and Lindqvist, Y. (1993) Role of tyrosine 129 in the active site of spinach glycolate oxidase, *Eur. J. Biochem. 213*, 1047−54.
7. Wagner, M. A., Trickey, P., Chen, Z. W., Mathews, F. S., and Jorns, M. S. (2000) Monomeric sarcosine oxidase: 1. Flavin reactivity and active site binding determinants, *Biochemistry 39*, 8813−24.
8. Ohta-Fukuyama, M., Miyake, Y., Emi, S., and Yamano, T. (1980) Identification and properties of the prosthetic group of choline oxidase from *Alcaligenes sp.*, *J. Biochem. 88*, 197−203.
9. Gomez-Moreno, C., Choy, M., and Edmondson, D. E. (1979) Purification and properties of the bacterial flavoprotein:thiamin dehydrogenase, *J. Biol. Chem. 254*, 7630−5.
10. Brühmuller, M., Möhler, H., and Decker, K. (1972) Covalently bound flavin in D-6-hydroxynicotine oxidase from *Arthrobacter oxidans*, *Z. Naturforsch., B 27*, 1073−4.
11. Gadda, G., Wels, G., Pollegioni, L., Zucchelli, S., Ambrosius, D., Pilone, M. S., and Ghisla, S. (1997) Characterization of cholesterol oxidase from *Streptomyces hygroscopicus* and *Brevibacterium sterolicum*, *Eur. J. Biochem. 250*, 369−76.
12. Müller, F., and Massey, V. (1969) Flavin-sulfite complexes and their structures, *J. Biol. Chem. 244*, 4007−16.
13. Gadda, G., and Fitzpatrick, P. F. (1998) Biochemical and physical characterization of the active FAD-containing form of nitroalkane oxidase from *Fusarium oxysporum*, *Biochemistry 37*, 6154−64.
14. Ghisla, S., Massey, V., and Yagi, K. (1986) Preparation and some properties of 6-substituted flavins as active site probes for flavin enzymes, *Biochemistry 25*, 3282−9.
15. Massey, V., and Ghisla, S. (1983) in *Biological Oxidations* (Sund, H., and Ullrich, V., Eds.) pp 114−39, Springer, Berlin.
16. Mayhew, S. G., Whitfield, C. D., Ghisla, S., and Schuman-Jorns, M. (1974) Identification and properties of new flavins in electron-transferring flavoprotein from *Peptostreptococcus elsdenii* and pig-liver glycolate oxidase, *Eur. J. Biochem. 44*, 579−91.
17. Müller, F., Ghisla, S., and Bacher, A. (1986) in *Wasserlösliche Vitamine* (Isler, O., Brubacher, G., and Ghisla, S., Eds.) Thieme, Stuttgart, Germany.
18. Fraaije, M. W., and Mattevi, A. (2000) Flavoenzymes: Diverse catalysts with recurrent features, *Trends Biochem. Sci. 25*, 126−32.
19. Trimmer, E. E., Ballou, D. P., Galloway, L. J., Scannell, S. A., Brinker, D. R., and Casas, K. R. (2005) Aspartate 120 of *Escherichia coli* Methylenetetrahydrofolate Reductase: Evidence for Major Roles in Folate Binding and Catalysis and a Minor Role in Flavin Reactivity, *Biochemistry 44*, 6809−22.
20. Mewies, M., Packman, L. C., Mathews, F. S., and Scrutton, N. S. (1996) Flavinylation in wild-type trimethylamine dehydrogenase and differentially charged mutant enzymes: A study of the protein environment around the N1 of the flavin isoalloxazine, *Biochem. J. 317*, 267−72.
21. Hecht, H. J., Hendle, J., Schmid, R. D., and Schomburg, D. (1993) Crystal structure of glucose oxidase from *Aspergillus niger* refined at 2.3 Å resolution, *J. Mol. Biol. 229*, 153−72.
22. Wohlfahrt, G., Witt, S., Hendle, J., Schomburg, D., Kalisz, H. M., and Hecht, H. J. (1999) 1.8 and 1.9 Å resolution structures of the *Penicillium amagasakiense* and *Aspergillus niger* glucose oxidases as a basis for modelling substrate complexes, *Acta Crystallogr. D55*, 969−77.
23. Vrielink, A., Lloyd, L. F., and Blow, D. M. (1991) Crystal structure of cholesterol oxidase from *Brevibacterium sterolicum* refined at 1.8 Å resolution, *J. Mol. Biol. 219*, 533−54.
24. Lario, P. I., Sampson, N., and Vrielink, A. (2003) Sub-atomic resolution crystal structure of cholesterol oxidase: What atomic resolution crystallography reveals about enzyme mechanism and the role of the FAD cofactor in redox activity, *J. Mol. Biol. 326*, 1635−50.
25. Yue, Q. K., Kass, I. J., Sampson, N. S., and Vrielink, A. (1999) Crystal structure determination of cholesterol oxidase from

Streptomyces and structural characterization of key active site mutants, *Biochemistry 38*, 4277−86.
26. Bannwarth, M., Bastian, S., Heckmann-Pohl, D., Giffhorn, F., and Schulz, G. E. (2004) Crystal structure of pyranose 2-oxidase from the white-rot fungus *Peniophora* sp., *Biochemistry 43*, 11683−90.
27. Hallberg, B. M., Leitner, C., Haltrich, D., and Divne, C. (2004) Crystal structure of the 270 kDa homotetrameric lignin-degrading enzyme pyranose 2-oxidase, *J. Mol. Biol. 341*, 781−96.
28. Hallberg, B. M., Henriksson, G., Pettersson, G., and Divne, C. (2002) Crystal structure of the flavoprotein domain of the extracellular flavocytochrome cellobiose dehydrogenase, *J. Mol. Biol. 315*, 421−34.
29. Xia, Z. X., and Mathews, F. S. (1990) Molecular structure of flavocytochrome b_2 at 2.4 Å resolution, *J. Mol. Biol. 212*, 837−63.
30. Lindqvist, Y., and Brändén, C. I. (1989) The active site of spinach glycolate oxidase, *J. Biol. Chem. 264*, 3624−8.
31. Mattevi, A., Vanoni, M. A., Todone, F., Rizzi, M., Teplyakov, A., Coda, A., Bolognesi, M., and Curti, B. (1996) Crystal structure of D-amino acid oxidase: A case of active site mirror-image convergent evolution with flavocytochrome b_2, *Proc. Natl. Acad. Sci. U.S.A. 93*, 7496−501.
32. Trickey, P., Wagner, M. A., Jorns, M. S., and Mathews, F. S. (1999) Monomeric sarcosine oxidase: Structure of a covalently flavinylated amine oxidizing enzyme, *Struct. Folding Des. 7*, 331−45.
33. Lim, L. W., Shamala, N., Mathews, F. S., Steenkamp, D. J., Hamlin, R., and Xuong, N. H. (1986) Three-dimensional structure of the iron−sulfur flavoprotein trimethylamine dehydrogenase at 2.4-Å resolution, *J. Biol. Chem. 261*, 15140−6.
34. Rowland, P., Bjornberg, O., Nielsen, F. S., Jensen, K. F., and Larsen, S. (1998) The crystal structure of *Lactococcus lactis* dihydroorotate dehydrogenase A complexed with the enzyme reaction product throws light on its enzymatic function, *Protein Sci. 7*, 1269−79.
35. Müh, U., Massey, V., and Williams, C. H., Jr. (1994) Lactate monooxygenase. I. Expression of the mycobacterial gene in *Escherichia coli* and site-directed mutagenesis of lysine 266, *J. Biol. Chem. 269*, 7982−8.
36. Burg, M. B., Kwon, E. D., and Kultz, D. (1997) Regulation of gene expression by hypertonicity, *Annu. Rev. Physiol. 59*, 437−55.
37. McNeil, S. D., Nuccio, M. L., and Hanson, A. D. (1999) Betaines and related osmoprotectants. Targets for metabolic engineering of stress resistance, *Plant Physiol. 120*, 945−50.
38. Fan, F., Ghanem, M., and Gadda, G. (2004) Cloning, sequence analysis, and purification of choline oxidase from *Arthrobacter globiformis*: A bacterial enzyme involved in osmotic stress tolerance, *Arch. Biochem. Biophys. 421*, 149−58.
39. Fan, F., and Gadda, G. (2005) On the catalytic mechanism of choline oxidase, *J. Am. Chem. Soc. 127*, 2067−74.
40. Ghanem, M., Fan, F., Francis, K., and Gadda, G. (2003) Spectroscopic and kinetic properties of recombinant choline oxidase from *Arthrobacter globiformis*, *Biochemistry 42*, 15179−88.
41. Fan, F., and Gadda, G. (2005) Oxygen- and temperature-dependent kinetic isotope effects in choline oxidase: Correlating reversible hydride transfer with environmentally enhanced tunneling, *J. Am. Chem. Soc. 127*, 17954−61.
42. Gadda, G. (2003) Kinetic mechanism of choline oxidase from *Arthrobacter globiformis*, *Biochim. Biophys. Acta 1646*, 112−8.
43. Gadda, G. (2003) pH and deuterium kinetic isotope effects studies on the oxidation of choline to betaine-aldehyde catalyzed by choline oxidase, *Biochim. Biophys. Acta 1650*, 4−9.
44. Gadda, G., Powell, N. L., and Menon, P. (2004) The trimethylammonium headgroup of choline is a major determinant for substrate binding and specificity in choline oxidase, *Arch. Biochem. Biophys. 430*, 264−73.
45. Ghanem, M., and Gadda, G. (2005) On the catalytic role of the conserved active site residue His466 of choline oxidase, *Biochemistry 44*, 893−904.
46. Whitby, L. G. (1953) A new method for preparing flavin-adenine dinucleotide, *Biochem. J. 54*, 437−42.
47. Corrado, M. E., Aliverti, A., Zanetti, G., and Mayhew, S. G. (1996) Analysis of the oxidation−reduction potentials of recombinant ferredoxin-$NADP^+$ reductase from spinach chloroplasts, *Eur. J. Biochem. 239*, 662−7.
48. Ghisla, S., Massey, V., Lhoste, J. M., and Mayhew, S. G. (1974) Fluorescence and optical characteristics of reduced flavines and flavoproteins, *Biochemistry 13*, 589−97.
49. Yalloway, G. N., Mayhew, S. G., Malthouse, J. P., Gallagher, M. E., and Curley, G. P. (1999) pH-dependent spectroscopic changes associated with the hydroquinone of FMN in flavodoxins, *Biochemistry 38*, 3753−62.
50. Massey, V., and Ganther, H. (1965) On the interpretation of the absorption spectra of flavoproteins with special reference to D-amino acid oxidase, *Biochemistry 4*, 1161−73.
51. Ackrell, B. A., Cochran, B., and Cecchini, G. (1989) Interactions of oxaloacetate with *Escherichia coli* fumarate reductase, *Arch. Biochem. Biophys. 268*, 26−34.
52. Ackrell, B. A., Kearney, E. B., and Edmondson, D. (1975) Mechanism of the reductive activation of succinate dehydrogenase, *J. Biol. Chem. 250*, 7114−9.
53. Barber, M. J., Pollock, V., and Spence, J. T. (1988) Microcoulometric analysis of trimethylamine dehydrogenase, *Biochem. J. 256*, 657−9.
54. Efimov, I., Cronin, C. N., and McIntire, W. S. (2001) Effects of noncovalent and covalent FAD binding on the redox and catalytic properties of *p*-cresol methylhydroxylase, *Biochemistry 40*, 2155−66.
55. Fraaije, M. W., van den Heuvel, R. H., van Berkel, W. J., and Mattevi, A. (1999) Covalent flavinylation is essential for efficient redox catalysis in vanillyl-alcohol oxidase, *J. Biol. Chem. 274*, 35514−20.
56. Meyer, T. E., Bartsch, R. G., Caffrey, M. S., and Cusanovich, M. A. (1991) Redox potentials of flavocytochromes c from the phototrophic bacteria, *Chromatium vinosum* and *Chlorobium thiosulfatophilum*, *Arch. Biochem. Biophys. 287*, 128−34.
57. Fan, F., Germann, M. W., and Gadda, G. (2006) Mechanistic studies of choline oxidase with betaine aldehyde and its isosteric analog 3,3-dimethylbutyraldehyde, *Biochemistry 45*, in press.
58. Engst, S., Kuusk, V., Efimov, I., Cronin, C. N., and McIntire, W. S. (1999) Properties of *p*-cresol methylhydroxylase flavoprotein overproduced by *Escherichia coli*, *Biochemistry 38*, 16620−8.
59. Khanna, P., and Jorns, M. S. (2003) Tautomeric rearrangement of a dihydroflavin bound to monomeric sarcosine oxidase or *N*-methyltryptophan oxidase, *Biochemistry 42*, 864−9.
60. Kim, J., Fuller, J. H., Kuusk, V., Cunane, L., Chen, Z. W., Mathews, F. S., and McIntire, W. S. (1995) The cytochrome subunit is necessary for covalent FAD attachment to the flavoprotein subunit of *p*-cresol methylhydroxylase, *J. Biol. Chem. 270*, 31202−9.
61. Mewies, M., McIntire, W. S., and Scrutton, N. S. (1998) Covalent attachment of flavin adenine dinucleotide (FAD) and flavin mononucleotide (FMN) to enzymes: The current state of affairs, *Protein Sci. 7*, 7−20.
62. Motteran, L., Pilone, M. S., Molla, G., Ghisla, S., and Pollegioni, L. (2001) Cholesterol oxidase from *Brevibacterium sterolicum*. The relationship between covalent flavinylation and redox properties, *J. Biol. Chem. 276*, 18024−30.
63. Kass, I. J., and Sampson, N. S. (1998) Evaluation of the role of His447 in the reaction catalyzed by cholesterol oxidase, *Biochemistry 37*, 17990−8000.
64. Clark, W. M. (1960) *Oxidation−reduction potentials of organic systems*, Williams & Wilkins, Baltimore.

BI052514M